Heliyon 9 (2023) e20300

Contents lists available at ScienceDirect

Heliyon

journal homepage: www.cell.com/heliyon

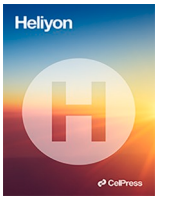

Design, synthesis, anticancer activity and docking studies of novel quinazoline-based thiazole derivatives as EGFR kinase inhibitors

M.S. Raghu [a], H.A. Swarup [b], T. Shamala [b], B.S. Prathibha [b], K. Yogesh Kumar [c,**], Fahd Alharethy [d], M.K. Prashanth [b,*], Byong-Hun Jeon [e,***]

[a] *Department of Chemistry, New Horizon College of Engineering, Bengaluru, 560 103, India*
[b] *Department of Chemistry, B N M Institute of Technology, Bengaluru, 560 070, India*
[c] *Department of Chemistry, Faculty of Engineering and Technology, Jain University, Ramanagara, 562 112, India*
[d] *Department of Chemistry, College of Science, King Saud University, Riyadh, 11451, Saudi Arabia*
[e] *Department of Earth Resources and Environmental Engineering, Hanyang University, 222, Wangsimni-ro, Seongdong-gu, Seoul, 04763, Republic of Korea*

ARTICLE INFO

Keywords:
Quinazoline
Thiazole
Anticancer
EGFR
Molecular docking

ABSTRACT

The *in vitro* anticancer efficacy of a new series of quinazoline-based thiazole derivatives was explored. Three cancer cell lines, MCF-7, HepG2, and A548, as well as the normal Vero cell lines, were tested employing the synthesized quinazoline-based thiazole compounds (4a-j). All of these compounds showed a moderate to significant cytotoxic impact that would have been noticeable and, in some cases, much more pronounced than the widely used drug erlotinib. For the MCF-7, HepG2, and A549 cell lines, respectively, the IC_{50} values of compound 4i were 2.86, 5.91, and 14.79 μM while those of compound 4j were 3.09, 6.87, and 17.92 μM. For their *in vitro* inhibitory effects against different EGFR kinases, such as the wild-type, L858R/T790 M, and L858R/T790 M/C797S, all the synthesized compounds were tested. The IC_{50} values for compound 4f against the wild-type, L858R/T790 M, and L858R/T790 M/C797S mutant EGFR kinases were 2.17, 2.81, and 3.62 nM, respectively. Investigations on the molecular docking of significant molecules indicated potential mechanisms of binding into the EGFR kinase active sites. By using in-silico simulations, compounds' putative drug-like qualities were verified. Finally, it has been shown that the newly synthesized compounds 4i and 4j are good candidates and beneficial for future design, optimization, and research to build more potent and selective EGFR kinase inhibitors with higher anticancer activity.

1. Introduction

The majority of fatalities worldwide are linked to cancer; hence, it is crucial to continue developing new antitumor drugs with high efficacy [1]. It is generally recognized that receptor tyrosine kinases are important protein signalling regulators for a variety of cellular activities, including those connected to cancer. Tyrosine kinase inhibitors (TKI) are currently widely used in the treatment of cancer

* Corresponding author.
** Corresponding author.
*** Corresponding author.
E-mail addresses: yogeshkk3@gmail.com (K.Y. Kumar), prashanthmk87@gmail.com (M.K. Prashanth), bhjeon@hanyang.ac.kr (B.-H. Jeon).

https://doi.org/10.1016/j.heliyon.2023.e20300
Received 19 December 2022; Received in revised form 26 August 2023; Accepted 18 September 2023
Available online 20 September 2023

and have received approval as anticancer medications [2]. The epidermal growth factor receptor (EGFR), a protein tyrosine kinase, has emerged as a crucial and primary target for the development of novel anticancer medications [3]. The ErbB family of transmembrane receptor tyrosine kinases includes the EGFR kinase, which controls the signalling pathways for cell migration, adhesion, proliferation, differentiation, and survival [4]. Inhibiting EGFR kinase in the treatment of cancer involves using small molecules to block this enzyme. The most popular treatments for non-small-cell lung cancer patients (NSCLC) are EGFR-TKI. As a result, one of the alluring targets for cancer therapy is the EGFR. Different small molecular EGFR inhibitors have been created through pharmacological development as treatment therapies for NSCLC. These medications raise concerns due to their developed drug resistance and significant adverse effects [5,6]. For instance, erlotinib markedly decreased the quantities of haemoglobin, white blood cells, and red blood cells. It harmed the internal organs and raised alanine aminotransferase levels and liver function indicators [7]. Similar to this, unusual hematologic side effects were discovered after erlotinib was given to individuals with advanced NSCLC [8]. Therefore, there is a compelling need to identify a new family of EGFR inhibitors with enhanced effectiveness but reduced toxicity.

Recently, the concept of molecular hybridization has become a potent method for finding new drugs [9]. In recent years, the discovery of novel medicines that can function as multitarget ligands for the treatment of cancer disorders has relied heavily on molecular hybridization based on the combination of pharmacophoric moieties [10,11]. In this regard, medicinal chemists are particularly interested in molecular hybrids that combine the pharmacophore quinazolinone with thiazole molecules. The most significant categories of heterocyclic chemicals in terms of pharmacology are quinazolines [12]. Due to the quinazolinone nucleus' stability, medicinal chemists have been motivated to add a variety of bioactive moieties to create novel potential therapeutic medicines [13–16]. Due to its wide range of biological activity, the quinazolinone skeleton is a commonly encountered heterocycle in the drug development process [17]. Another significant pharmacophore in medicinal chemistry is thiazoles. They are one of the most significant prospective moieties in the chemical world of thiazole-containing compounds that are constantly expanding and exhibiting noticeable pharmacological activities [18]. The thiazole moiety has been crucial in drug development due to its structural characteristics and significance in several biological activities [19,20]. In addition, a variety of pharmaceutical compounds that include quinazoline (gefitinib, lapatinib, erlotinib and afatinib) and thiazole (dasatinib) motifs have been proven to be effective EGFR inhibitors, as shown in Fig. 1.

Aiming to combine two bioactive entities, quinazoline and thiazole, into a single compact hybrid structure to create EGFR kinase inhibitors, the current work was motivated by all of these facts and continued our earlier efforts to plot and synthesize new therapeutic agents [21–30]. As EGFR-mutant kinase inhibitors for the treatment of NSCLC human breast (MCF-7), liver (HepG2), and lung (A549) cancer cell lines, we developed and synthesized new quinazoline-based thiazole compounds.

2. Experimental

2.1. Materials

The chemical reagents and solvents employed in the experiment were all commercially purchased. Using Bruker Advance equipment, ^{1}H (400 MHz) and ^{13}C NMR (100 MHz) data were obtained. A PerkinElmer LC-MS PE Sciex API/65 Spectrophotometer was used to record mass spectra. The Buchi 530 Melting Point Device is used to test the melting point. A PerkinElmer type 240 C analyzer was used to do elemental analysis. TLC plates pre-coated by Merck were utilized.

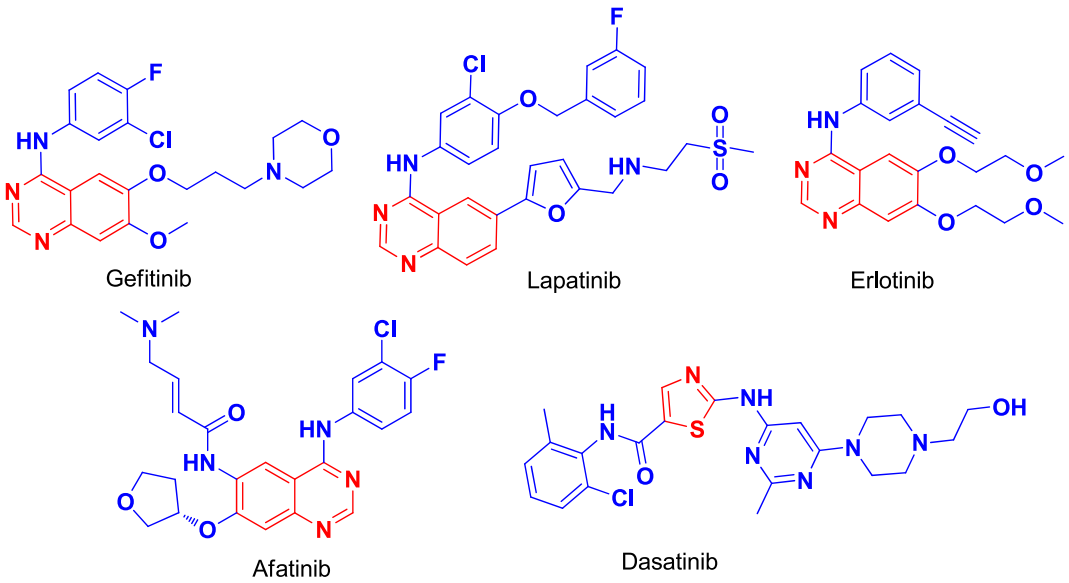

Fig. 1. Structures of marketed quinazoline (gefitinib, lapatinib, erlotinib and afatinib) and thiazole-based (dasatinib) EGFR inhibitors.

2.2. Synthesis of 1-(4-hydroxyquinazolin-7-yl)thiourea (2)

Dropwise addition of HCl (10 mmol) was done to a stirred solution of 7-aminoquinazolin-4-ol (5 mmol) and ammonium thiocyanate (5 mmol) in ethanol (15 mL). After the dropwise addition was completed, the reaction mixture was refluxed for 6 h. The solid product produced after the reaction was completed was filtered, washed with water, dried, and recrystallized from ethanol to obtain compound 2. Yield: 91%. Anal. calc. for $C_9H_8N_4OS$: C, 49.08; H, 3.66; N, 25.44. found: C, 49.05; H, 3.62; N, 25.49. ^{1}H NMR (400 MHz, $CDCl_3$) δ: 5.28 (s, 1H), 7.02 (d, 1H), 7.32 (s, 1H), 7.58 (d, 1H), 8.46 (s, 1H), 8.91 (s, 2H), 11.28 (s, 1H). MS, *m/z*: 221 (M+1).

2.3. Synthesis of compounds 4a-j

2 mmol of substituted bromoacetophenone (3a-j) was added to compound 2 (2 mmol) in ethanol (10 mL). Triethylamine (2.2 mmol) was added to this mixture, and the reaction mixture was refluxed for 8 h. The reaction mixture was quenched in water and extracted with dichloromethane when the reaction was complete. The organic portion was dried over anhydrous Na_2SO_4, concentrated in vacuo, and recrystallized from ethanol to yield 4a-j.

2.3.1. 7-((4-Phenylthiazol-2-yl)amino)quinazolin-4-ol (4a)

Yield: 91%. mp.: 221–223 °C. Anal. calc. for $C_{17}H_{12}N_4OS$: C, 63.73; H, 3.78; N, 17.49. found: C, 63.71; H, 3.75; N, 17.54. ^{1}H NMR (400 MHz, DMSO-d_6) δ: 5.21 (s, 1H), 7.16 (d, 1H, J = 8.4 Hz), 7.28 (s, 1H), 7.41 (s, 1H), 7.49–7.51 (m, 1H), 7.62–7.64 (m, 2H), 7.80 (d, 1H, J = 7.2 Hz), 8.07 (d, 2H, J = 6.4 Hz), 8.50 (s, 1H), 11.26 (s, 1H). ^{13}C NMR (100 MHz, DMSO-d_6) δ: 105.1, 107.6, 108.9, 119.3, 120.5, 127.5, 128.7, 129.2, 133.1, 150.2, 150.6, 151.3, 155.2, 160.6, 177.8. MS, *m/z*: 321 (M+1).

2.3.2. 7-((4-(p-tolyl)thiazol-2-yl)amino)quinazolin-4-ol (4b)

Yield: 87%. mp.: 236–238 °C. Anal. calc. for $C_{18}H_{14}N_4OS$: C, 64.65; H, 4.22; N, 16.75. found: C, 64.63; H, 4.21; N, 16.78. ^{1}H NMR (400 MHz, DMSO-d_6) δ: 2.36 (s, 3H), 5.21 (s, 1H), 7.15 (d, 1H, J = 7.6 Hz), 7.32 (s, 1H), 7.45 (s, 1H), 7.71 (d, 1H, J = 5.6 Hz), 8.08 (d, 2H, J = 6.4 Hz), 8.17 (d, 2H, J = 6.0 Hz), 8.47 (s, 1H), 11.25 (s, 1H). ^{13}C NMR (100 MHz, DMSO-d_6) δ: 21.3, 105.3, 107.6, 108.9, 119.3, 120.6, 125.7, 129.5, 130.1, 131.7, 150.2, 150.6, 151.3, 155.1, 160.6, 177.8. MS, *m/z*: 335 (M+1).

2.3.3. 7-((4-(4-hydroxyphenyl)thiazol-2-yl)amino)quinazolin-4-ol (4c)

Yield: 90%. mp.: 227–229 °C. Anal. calc. for $C_{17}H_{12}N_4O_2S$: C, 60.70; H, 3.60; N, 16.66. found: C, 60.67; H, 3.58; N, 16.69. ^{1}H NMR (400 MHz, DMSO-d_6) δ: 5.23 (s, 1H), 5.58 (s, 1H), 7.11 (d, 1H, J = 7.8 Hz), 7.36 (s, 1H), 7.42 (s, 1H), 7.68 (d, 1H, J = 6.3 Hz), 8.06 (d, 2H, J = 6.8 Hz), 8.15 (d, 2H, J = 6.4 Hz), 8.43 (s, 1H), 11.27 (s, 1H). ^{13}C NMR (100 MHz, DMSO-d_6) δ: 105.3, 107.6, 108.9, 116.4, 119.3, 120.6, 125.6, 128.9, 150.3, 150.6, 151.3, 155.1, 158.5, 160.6, 177.8. MS, *m/z*: 337 (M+1).

2.3.4. 7-((4-(4-methoxyphenyl)thiazol-2-yl)amino)quinazolin-4-ol (4d)

Yield: 90%. mp.: 232–234 °C. Anal. calc. for $C_{18}H_{14}N_4O_2S$: C, 61.70; H, 4.03; N, 15.99. found: C, 61.67; H, 4.01; N, 16.03. ^{1}H NMR (400 MHz, DMSO-d_6) δ: 3.86 (s, 3H), 5.28 (s, 1H), 7.02 (d, 1H, J = 9.2 Hz), 7.33 (s, 1H), 7.55 (d, 1H, J = 6.8 Hz), 7.65 (s, 1H), 8.08 (d, 2H, J = 6.4 Hz), 8.15 (d, 2H, J = 6.2 Hz), 8.55 (s, 1H), 11.25 (s, 1H). ^{13}C NMR (100 MHz, DMSO-d_6) δ: 55.8, 105.2, 107.5, 108.9, 114.8, 119.3, 120.6, 125.3, 128.5, 150.3, 150.6, 151.3, 155.1, 160.6, 160.8, 177.6. MS, *m/z*: 351 (M+1).

2.3.5. 7-((4-(4-aminophenyl)thiazol-2-yl)amino)quinazolin-4-ol (4e)

Yield: 86%. mp.: 229–231 °C. Anal. calc. for $C_{17}H_{13}N_5OS$: C, 60.88; H, 3.91; N, 20.88. found: C, 60.85; H, 3.89; N, 20.94. ^{1}H NMR (400 MHz, DMSO-d_6) δ: 5.23 (s, 1H), 6.28 (s, 2H), 7.13 (d, 1H, J = 7.8 Hz), 7.29 (s, 1H), 7.48 (s, 1H), 7.64 (d, 1H, J = 7.2 Hz), 7.95 (d, 2H, J = 6.4 Hz), 8.16 (d, 2H, J = 7.6 Hz), 8.48 (s, 1H), 11.28 (s, 1H). ^{13}C NMR (100 MHz, DMSO-d_6) δ: 105.1, 107.6, 108.9, 119.3, 120.5, 128.3, 115.1, 123.2, 145.6, 150.2, 150.6, 151.3, 155.2, 160.6, 177.8. MS, *m/z*: 336 (M+1).

2.3.6. 7-((4-(4-fluorophenyl)thiazol-2-yl)amino)quinazolin-4-ol (4f)

Yield: 88%. mp.: 211–213 °C. Anal. calc. for $C_{17}H_{11}F_4N_4OS$: C, 60.34; H, 3.28; N, 16.56. found: C, 60.32; H, 3.25; N, 16.59. ^{1}H NMR (400 MHz, DMSO-d_6) δ: 5.23 (s, 1H), 7.04 (d, 1H, J = 8.6 Hz), 7.35 (s, 1H), 7.44 (s, 1H), 7.55 (d, 1H, J = 8.1 Hz), 8.07 (d, 2H, J = 6.8 Hz), 8.15 (d, 2H, J = 6.2 Hz), 8.45 (s, 1H), 11.28 (s, 1H). ^{13}C NMR (100 MHz, DMSO-d_6) δ: 105.2, 107.6, 108.9, 116.2, 119.3, 120.6, 128.6, 130.6, 150.1, 150.6, 151.3, 155.1, 160.6, 162.9, 177.7. MS, *m/z*: 339 (M+1).

2.3.7. .7-((4-(4-chlorophenyl)thiazol-2-yl)amino)quinazolin-4-ol (4g)

Yield: 85%. mp.: 216–218 °C. Anal. calc. for $C_{17}H_{11}ClN_4OS$: C, 57.55; H, 3.12; N, 15.79. found: C, 57.53; H, 3.11; N, 15.83. ^{1}H NMR (400 MHz, DMSO-d_6) δ: 5.22 (s, 1H), 7.08 (d, 1H, J = 8.2 Hz), 7.39 (s, 1H), 7.41 (s, 1H), 7.63 (d, 1H, J = 7.6 Hz), 8.06 (d, 2H, J = 6.9 Hz), 8.17 (d, 2H, J = 6.3 Hz), 8.44 (s, 1H), 11.26 (s, 1H). ^{13}C NMR (100 MHz, DMSO-d_6) δ: 105.3, 107.5, 108.9, 119.3, 120.6, 128.9, 129.3, 131.1, 134.3, 150.2, 150.6, 151.3, 155.1, 160.6, 177.8. MS, *m/z*: 355 (M+1).

2.3.8. 7-((4-(4-bromophenyl)thiazol-2-yl)amino)quinazolin-4-ol (4h)

Yield: 87%. mp.: 218–220 °C. Anal. calc. for $C_{17}H_{11}BrN_4OS$: C, 51.14; H, 2.78; N, 14.03. found: C, 51.12; H, 2.75; N, 14.08. ^{1}H NMR (400 MHz, DMSO-d_6) δ: 5.25 (s, 1H), 7.14 (d, 1H, J = 7.8 Hz), 7.24 (s, 1H), 7.52 (s, 1H), 7.69 (d, 1H, J = 7.2 Hz), 7.98 (d, 2H, J = 6.4 Hz), 8.17 (d, 2H, J = 7.6 Hz), 8.51 (s, 1H), 11.27 (s, 1H). ^{13}C NMR (100 MHz, DMSO-d_6) δ: 105.1, 107.6, 108.9, 119.3, 120.5, 128.3,

132.2, 132.8, 123.7, 150.2, 150.6, 151.3, 155.2, 160.6, 177.8. MS, *m/z*: 400 (M+1).

2.3.9. 7-((4-(4-(trifluoromethyl)phenyl)thiazol-2-yl)amino)quinazolin-4-ol (4i)

Yield: 87%. mp.: 223–225 °C. Anal. calc. for $C_{18}H_{11}F_3N_4OS$: C, 55.67; H, 2.85; N, 14.43. found: C, 55.65; H, 2.81; N, 14.48. ^{1}H NMR (400 MHz, DMSO-d_6) δ: 5.26 (s, 1H), 7.02 (d, 1H, $J = 9.2$ Hz), 7.34 (s, 1H), 7.44 (s, 1H), 7.52 (d, 1H, $J = 8.4$ Hz), 8.08 (d, 2H, $J = 6.3$ Hz), 8.16 (d, 2H, $J = 5.6$ Hz), 8.47 (s, 1H), 11.24 (s, 1H). ^{13}C NMR (100 MHz, DMSO-d_6) δ: 105.2, 107.5, 108.9, 119.3, 120.6, 124.1, 125.6, 126.1, 131.2, 136.3, 150.3, 150.6, 151.3, 155.1, 160.6, 177.8. MS, *m/z*: 389 (M+1).

2.3.10. 7-((4-(4-nitrophenyl)thiazol-2-yl)amino)quinazolin-4-ol (4j)

Yield: 92%. mp.: 242–244 °C. Anal. calc. for $C_{17}H_{11}N_5O_3S$: C, 55.88; H, 3.03; N, 19.17. found: C, 55.85; H, 3.01; N, 19.19. ^{1}H NMR (400 MHz, DMSO-d_6) δ: 5.21 (s, 1H), 7.09 (d, 1H, $J = 7.2$ Hz), 7.33 (s, 1H), 7.41 (s, 1H), 7.58 (d, 1H, $J = 7.9$ Hz), 8.07 (d, 2H, $J = 5.3$ Hz), 8.18 (d, 2H, $J = 7.2$ Hz), 8.46 (s, 1H), 11.23 (s, 1H). ^{13}C NMR (100 MHz, DMSO-d_6) δ: 105.2, 107.6, 108.9, 119.3, 120.6, 124.4, 126.2, 139.1, 147.9, 150.2, 150.6, 151.3, 155.1, 160.6, 177.8. MS, *m/z*: 366 (M+1).

2.4. Cytotoxic activity

The MTT assay, which is reported in the previous paper [31], was used to assess the cytotoxic activity of the synthesized compounds against the three cancer cell lines MCF-7 (human breast), HepG2 (human liver), and A549 (human lung) and the normal Vero cell line. A positive control, erlotinib, was utilized. In a nutshell, 1×10^5 cells per well were seeded three times in six-well plates containing exponentially developing cells. The cells were given an additional 24 h of treatment with all of the test substances at various doses. All wells received 20 μL of MTT (5 mg/mL) after 48 h of treatment, which was then incubated for 4 h at 37 °C. After that, each well received 40 μL of DMSO after the medium had been thoroughly removed. The ELISA plate reader was used to analyze the plates at a 595 nm wavelength. The concentration of molecules at which growth in various cell lines was 50% inhibited relative to the control culture is known as the IC_{50} of that compound.

2.5. EGFR kinase inhibition assay

The target compounds' abilities to inhibit the EGFR kinase were assessed using 96-well plates and the previously published enzyme-linked immunosorbent assays (ELISA) [32]. The IC_{50} values for each compound's EGFR kinase activity were reported. The IC_{50} values were determined using the Prism GraphPad program and nonlinear regression with a normalized dose-response fit. All data are provided as the mean ± SD of three separate experiments, and significant differences were taken into account if $P < 0.05$.

2.6. Molecular docking

Molecular docking using Autodock Vina was employed to estimate the various binding modes of all potent compounds with EGFR. The 3D structure of EGFR in combination with osimertinib (PDB ID: 6LUD) was retrieved from the protein data bank. Water molecules and repetitive chains were eliminated. Protons were added, and the protein's energy was reduced. To perform intermediary processes like producing pdbqt files for protein and ligand preparation and building grid boxes, the graphical user interface tool AutoDock Tools is employed. The docked findings are viewed and analyzed using the Discovery Studio Visualizer. The docking score and H-bond interactions were determined for all of the compounds utilized in this investigation. The molecular properties of the synthesized compounds were analyzed using the internet server http://www.swissadme.ch/to ensure compliance with the Lipinski rule of Five.

3. Results and discussion

3.1. Synthesis

In Scheme 1, the pathways for producing new quinazoline-based thiazole derivatives are described, and Table 1 displays the structures of the derivatives 4a-j. These compounds were obtained in two steps, which are detailed in the experimental section. ^{1}H NMR, ^{13}C NMR, mass spectra, and elemental analyses are used to identify each one, and the results are in good agreement with the structures that have been described (Supplementary file). To begin the process of producing 1-(4-hydroxyquinazolin-7-yl)thiourea (2), 7-aminoquinazolin-4-ol (1), and ammonium thiocyanate, they were condensed in an acidic environment. The production of thiourea

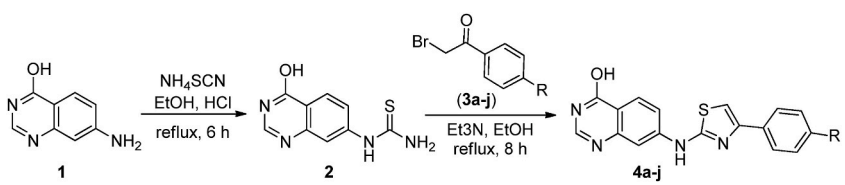

Scheme 1. Synthetic route for the preparation of target compounds 4a-j.

Table 1
Target compounds structure 4a-j.

Compound	R	Final structure
4a	-H	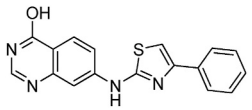
4b	-CH_3	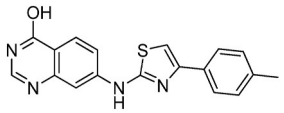
4c	-OH	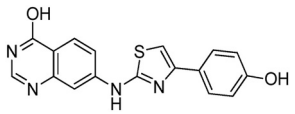
4d	-OCH_3	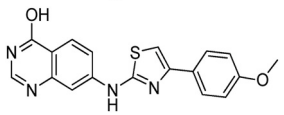
4e	-NH_2	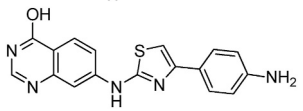
4f	-F	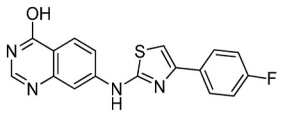
4g	-Cl	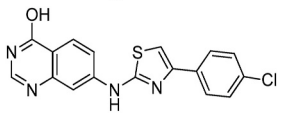
4h	-Br	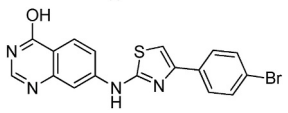
4i	-CF_3	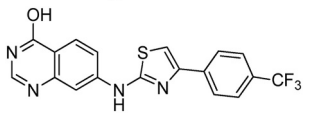
4j	-NO_2	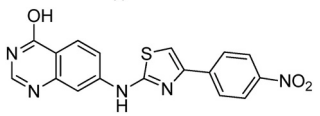

was confirmed by the ^{1}H NMR spectrum data of compound 2, which showed two singlet peaks at 5.28 ppm and 8.91 ppm, respectively, in the –NH and –NH_2 groups. The relevant target compounds 4a-j were produced by cyclo-condensing 1-(4-hydroxyquinazolin-7-yl) thiourea (2) under reflux with the substituted bromoacetophenones (3a-j) in ethanol in the presence of triethylamine. A comparison of the spectral data for compounds 2 and 4a-j showed that the singlet peak for the –NH_2 group had disappeared at 8.91 ppm and that a new singlet peak had appeared at 7.24–7.45 ppm in the target compound's ^{1}H NMR spectrum, thereby confirming the formation of the thiazole ring via cyclo-condensation reaction. The target compounds ^{1}H NMR spectra also revealed signals in the 5.21–5.28 ppm and 11.23–11.28 ppm ranges, which are indicative of the –NH and –OH groups, respectively. Compound synthesis was also assisted by the aromatic cluster of molecules. All newly synthesized compounds mass spectra had the M+1 peak, which is consistent with their chemical formula.

3.2. Antiproliferative activity

Using the MTT assay and erlotinib as a positive control, the newly synthesized compounds 4a-j were tested for their *in vitro* cytotoxicity against the MCF-7, HepG2, and A549 human cancer cell lines. Since cell lines are broadly applicable to many aspects of laboratory research and are particularly useful as *in vitro* models in cancer research, they appear to be a crucial component for the molecular diagnosis of cancer. MCF-7 cells are often utilized in research on the biology of tumors and the mechanism of action of

hormones in breast cancer [33]. HepG2 cells, on the other hand, are the most often investigated hepatic cell lines due to the benefits of human protein availability and secretion. HepG2 cells were the first to display the essential properties of hepatocytes. It is used for studying the cytotoxic effects of drugs, nanoparticles, and heavy metals *in vitro* [34]. Additionally, the A549 cells are epithelial cells that are useful for studying the metabolic processes of lung tissue and potential drug delivery mechanisms to the tissue. Likewise, the most popular human NSCL cancer cell line for drug discovery is A549 [35]. As a result, the MCF-7, HepG2, and A549 cell lines have been used in this investigation to evaluate the anti-proliferative activity of the compounds. The antiproliferative activity was expressed as the mean IC_{50} of three separate experiments and the standard deviation from three replicates after the 50% inhibitory concentration (IC_{50}) was determined. Even at 50 μM, all of the compounds were noncytotoxic in our cell viability testing against the non-tumorigenic Vero cell line. The findings of their cytotoxic activities are shown in Table 2.

The MCF-7 cell line was more responsive than the HepG2 and A549 cell lines, according to Table 2's findings. With IC_{50} values of 2.86, 5.91, and 14.79 μM, respectively, compound 4i demonstrated the strongest activity against the tested MCF-7, HepG2, and A549 cells when compared to the reference medication erlotinib. With an IC_{50} value of 3.09, 6.87, and 17.92 μM against the tested MCF-7, HepG2, and A549 cancer cell lines, respectively, compound 4j showed the second-highest activity. Additionally, compounds 4f, 4g and 4h had positive antiproliferative effects (IC_{50} values of 3.71, 7.92, and 19.02 μM, 4.14, 9.36, and 20.84 μM, 4.92, 9.85, and 22.86 μM, respectively). With IC_{50} values ranging from 6.21 to 31.16 μM, compounds 4a-e have modest activity against the cancer cell lines that have been examined. Compounds 4i and 4j, when compared to the reference medication erlotinib, demonstrated, 1.19- and 1.04-fold better antiproliferative potency against all cell lines, respectively.

3.3. Structure-activity relationship (SAR) study

Based on the results of the compounds 4a-j anti-proliferative activities, the preliminary SAR investigation was concluded. A face-to-edge aromatic contact between the quinazoline, thiazole, and phenyl moieties and the target sites are suggested by the fact that most of the compounds exhibited substantial anti-proliferative activity. Interestingly, compound 4i, which has a trifluoromethyl group in the fourth position of the aromatic ring, is superior to the other substituents in this series. In molecule 4j, the nitro group could represent a suitable candidate substituent that would strengthen its antiproliferative action. Compound 4i of this series, which has a hydroxy group in the fourth position of the quinazoline moiety and a trifluoromethyl group in the fourth position of the aromatic ring, has been shown to be crucial for activity. The anti-proliferative action significantly changed when the electronic nature of the substituent group attached to the aromatic ring was modified. The insertion of the electron-withdrawing groups (EWGs) at the 4th position of the phenyl ring (4f-j) demonstrated considerable anti-proliferative actions against all of the tested MCF-7, HepG2, and A549 cell lines in contrast to the unsubstituted (4a) at position number 4 of the phenyl nucleus. A decrease in anti-proliferative effects was also seen when the electron-donating groups (EDGs) were inserted into the phenyl nucleus at position 4 (4b-e). Overall, the nature of the substituents introduced to the fourth position of the phenyl ring attached to the thiazole nucleus had a considerable influence on anti-proliferative efficiency. These findings made it very evident that compounds 4i and 4j were the most effective against all cancer cell lines tested. We therefore think that these synthetic compounds are excellent options for cancer treatment since they can specifically target cancer cells.

3.4. EGFR kinase inhibitory activity

For the treatment of NSCLC patients with EGFR mutations in various clinical situations, three generations of EGFR-TKIs have now been approved. First-generation and second-generation EGFR-TKIs have shown significant therapeutic benefits in patients with advanced NSCLC, but they become ineffective when the EGFR mutation, an acquired mutation that results in drug resistance, manifests [36]. In patients with the EGFR mutation, Osimertinib, the third-generation EGFR inhibitor to be approved-can prolong progression-free survival by more than 10 months [37]. Although it has no effect on EGFR in its wild-type form, osimertinib has a high affinity for the drug-resistant L855R/T790 M double mutant. A tertiary mutation in the EGFR was also discovered in almost 40% of patients who underwent osimertinib treatment, according to clinical investigations [38]. This mutation prevented the irreversible inhibitors from forming a covalent bond with the side chain of C797. It is therefore necessary to find effective inhibitors of both the

Table 2
Cytotoxicity of compounds 4a-j on cancer cell lines.

Compound	IC_{50} (μM)			
	MCF-7	HepG2	A549	Vero
4a	6.21 ± 0.33	11.86 ± 0.71	24.73 ± 0.95	>50
4b	6.28 ± 0.58	12.59 ± 1.02	27.04 ± 1.09	>50
4c	7.43 ± 0.91	14.16 ± 0.83	31.16 ± 0.97	>50
4d	9.75 ± 1.03	17.28 ± 0.98	24.97 ± 1.14	>50
4e	8.29 ± 0.44	15.03 ± 0.81	29.61 ± 1.22	>50
4f	3.71 ± 0.47	7.92 ± 0.63	19.02 ± 0.83	>50
4g	4.14 ± 0.69	9.36 ± 1.15	20.84 ± 1.24	>50
4h	4.92 ± 0.31	9.85 ± 0.97	22.86 ± 1.06	>50
4i	2.86 ± 0.31	5.91 ± 0.45	14.79 ± 1.03	>50
4j	3.09 ± 0.45	6.87 ± 0.59	17.92 ± 0.95	>50
Erlotinib	3.16 ± 0.22	6.83 ± 0.51	19.42 ± 1.28	>30

EGFR mutant and wild-type. The L858R/T790 M, L858R/T790 M/C797S, and wild-type EGFR kinases were used to test the kinase inhibitory effects of quinazoline-based thiazole derivatives (4a-j). The positive controls consisted of approved EGFR kinases such as osimertinib, brigatinib, and staurosporine. Table 3 contains the compounds IC_{50} values for each test substance. The IC_{50} values for all of the target substances ranged from 2.17 to 16.32 nM, indicating strong inhibitory action against the EGFR-WT enzyme. As shown in Table 3, however, all of the target substances demonstrated moderate to exceptional inhibitory action against the dual-mutant and triple-mutant enzymes, with the IC_{50} values varying from 2.81 to 23.74 nM and 3.62–31.74 nM, respectively. Overall, the compounds in this series were more potent when R had a fluoro (4f), chloro (4g), bromo (4h), trifluoromethyl (4i), or nitro (4j) group than the comparable analogs with an unsubstituted (4a), methyl (4b), methoxy (4c), hydroxy (4d), or amine (4e) group. Comparatively to EDGs, these findings imply that EWGs were preferable for EGFR kinase inhibitory activity. These kinase test findings demonstrated that compound 4i had the strongest inhibitory action against the wild-type, L858R/T790 M, and L858R/T790 M/C797S EGFR mutants, demonstrating that the trifluoromethyl group was tolerated at the fourth position of the phenyl ring. The trifluoromethyl group may be best for the EGFR kinase inhibitory action, as evidenced by the findings of this study and our comparison of the data from 4a-j.

3.5. Molecular docking studies

One of the most fundamental and significant methods for drug design and discovery has been molecular docking studies. Dysregulation of protein kinases occurs frequently in cancer cells. A certain kind of receptor tyrosine kinase called EGFR is essential for controlling fundamental cellular functions. One of the most prevalent causes of the pathogenesis and development of NSCLC is EGFR overexpression or mutation [39]. NSCLC, metastatic colorectal cancer, glioblastoma, head and neck cancer, pancreatic cancer, and breast cancer have higher EGFR receptor tyrosine kinase levels [40]. Any EGFR malignancy can cause lung cancer to spread. When administered effectively, EGFR-TK inhibitors can lower the expression of signalling pathways downstream of EGFR kinases and demonstrably inhibit tumour cell growth [41,42]. As a result, EGFR-TK would be recognized as a promising and effective anticancer target. To do this, molecular docking utilizing Autodock Vina was used to mimic the contact and affinity of the newly synthesized compounds 4g, 4i, and 4j with the mutant EGFR kinase of L858R/T790 M/C797S (PDB ID: 6LUD). The extracted co-crystallized ligand osimertinib from the 3D structure 6LUD was redocked using the same methodology for the docked compounds as a first step in validating the docking protocol parameters. Fig. 2 (4g, 4i and 4j) and Fig. 3 (4g, 4i and 4j) depicts the predicted 3D and 2D interaction modes of potent compounds, respectively. Compounds 4g, 4i, and 4j had docking scores of −8.03, −8.49, and −8.26 kcal/mol, respectively, when they were docked into the active site of EGFR (Table 4). According to docking investigations, the compounds 4i and 4j docking scores are greater than the widely prescribed drug Osimertinib's docking score of −8.21 kcal/mol. The most active molecule, 4i, had three hydrogen bonding interactions with crucial amino acids, including Cys-781, Gly-857, and Thr-903. Additionally, the compound 4j backbone was securely stretched to create three π-alkyl connections with the protein residues Leu-747, Ile-759, and Val-786. Similar to compound 4i, where there are unambiguous π-alkyl contacts between the quinazolinone core and the amino acid residues Leu-747, Ile-759, and Val-786, compound 4g interacts in a similar way. Additionally, compound 4g form one hydrogen bond with Gly-857. Concerning compound 4j, the ligand formed two hydrogen bonds with Ile-759 and Gly-857, as well as two π-alkyl interactions with Val-786 and Leu-788. The results of the docking investigation complemented experimentally observed cytotoxic and EGFR kinase assessment data. The results of molecular docking, along with data from the antiproliferative and EGFR kinase inhibition experiments, indicate that compounds 4i and 4j might be employed as anticancer agents.

3.6. Drug-likeness properties

A general recommendation used to assess drug similarity is Lipinski's rule of five [43]. It helps establish whether a chemical molecule with a certain pharmacological or biological activity has chemical and physical characteristics that would make it likely to be an orally active medication in humans. Topological polar surface area (TPSA), octanol-water partition coefficient (logP), hydrogen

Table 3
EGFR kinase inhibition of compounds 4a-j.

Compound	EGFR Kinase IC_{50} (nM)		
	WT	LR/TM	LR/TM/CS
4a	10.01 ± 0.58	20.95 ± 0.86	25.49 ± 1.09
4b	8.59 ± 0.93	15.27 ± 0.81	19.62 ± 1.22
4c	16.32 ± 1.07	21.69 ± 1.04	25.09 ± 1.14
4d	10.06 ± 0.91	23.74 ± 0.74	31.74 ± 0.69
4e	14.19 ± 0.72	21.83 ± 1.02	29.35 ± 1.14
4f	5.16 ± 0.72	9.27 ± 0.60	15.38 ± 0.98
4g	4.81 ± 0.36	6.95 ± 0.58	13.14 ± 0.91
4h	4.96 ± 0.44	7.08 ± 0.51	13.06 ± 1.02
4i	2.17 ± 0.18	2.81 ± 0.44	3.62 ± 0.51
4j	2.93 ± 0.47	4.62 ± 0.21	7.59 ± 0.63
Staurosporine	391.65 ± 1.84	40.81 ± 1.03	3.92 ± 0.55
Brigatinib	35.72 ± 1.06	4.17 ± 0.59	1.63 ± 0.21
Osimertinib	5.01 ± 0.38	0.50 ± 0.06	410.73 ± 1.58

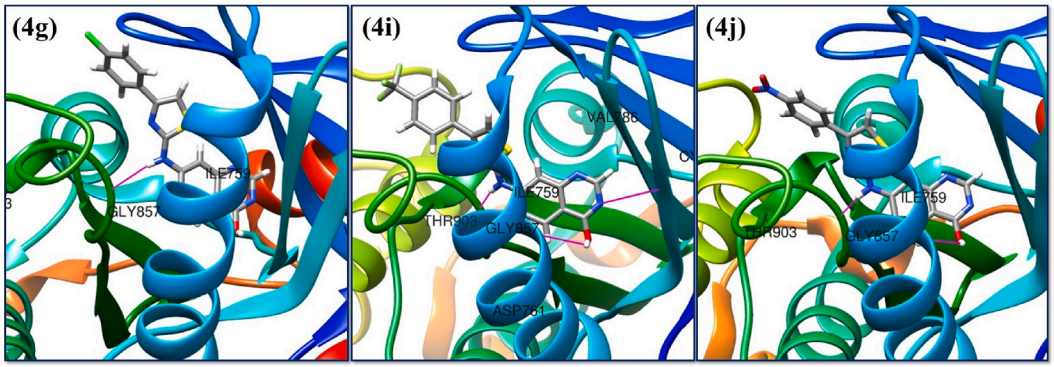

Fig. 2. Predicted binding mode of potent compounds 4g, 4i and 4j bound to target protein (PDB ID: 6LUD).

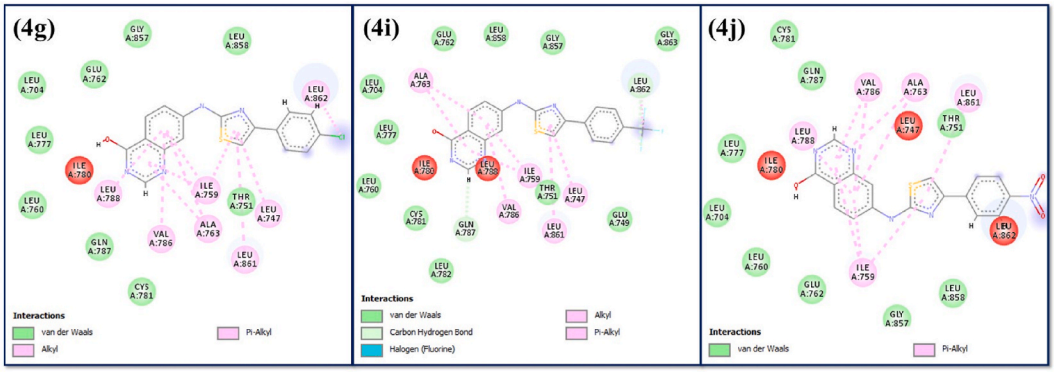

Fig. 3. 2D interactions of the potent compounds 4g, 4i and 4j bound to target protein (PDB ID: 6LUD).

Table 4
Analysis of molecular docking interaction of potent compounds 4g, 4i and 4j with target protein (PDB ID: 6LUD).

Compound	Docking score (kcal/mol)	Interacting residues		
		H-bond	Hydrophobic	π-alkyl
4g	−8.03	Gly-857	Leu-704, Thr-751, Leu-760, Glu-762, Ala-763, Leu-777, Cys-781, Leu-788, Leu-858, Leu-861, Gln-787, Leu-862	Leu-747, Ile-759, Val-786
4i	−8.49	Cys-781, Gly-857, Thr-903	Leu-704, Glu-749, Thr-751, Leu-760, Glu-762, Ala-763, Leu-777, Ile-780, Leu-782, Gln-787, Leu-788, Gly-857, Leu-858, Leu-862, Leu-861, Gly-863	Leu-747, Ile-759, Val-786
4j	−8.26	Ile-759, Gly-857	Leu-704, Leu-747, Thr-751, Leu-760, Glu-762, Ala-763, Leu-777, Ile-780, Cys-781, Gln-787, Leu-858, Leu-861, Leu-862	Val-786, Leu-788
Osimertinib	−8.21	Cys-781, Gly-857	Leu-704, Phe-723, Glu-749, Thr-751, Glu-762, Ala-763, Met-766, Leu-777, Ile-780, Leu-782, Thr-785, Gln-787, Leu-788, Gly-857, Leu-858, Leu-861, Gly-863, Ala-864	Leu-747, Ile-788, Leu-862

bond donors (HBD) and acceptors (HBA), and molecular weight (MW) are factors taken into account by this rule. Excellent descriptors of drug absorption, bioavailability, and permeability have been demonstrated to be LogP and TPSA [44]. As a result, we examined the synthetic compounds (4a-j) in silico to evaluate their drug-like characteristics. Using the SwissADME online property toolbox, the descriptors of Lipinski's rule of five were determined. The findings are shown in Table 5. The molecular weights of compounds 4a-j ranged from 320.37 to 399.26 Da, while Log P values ranged from 2.09 to 3.02; these values corroborated with those required by Lipinski's rule to create drug-like compounds. Notably, the synthesized compounds' anticipated HBA and HBD values fell within the permitted range. In addition, we determined the total polar surface area (TPSA), which has a significant impact on the bioavailability of medicines. Consequently, it is believed that drugs with TPSA >140 that are passively absorbed have limited oral bioavailability. Since the newly synthesized molecules 4a-j adhered to Lipinski's rule of five, it is feasible to employ the newly created quinazoline-based thiazole derivatives as safe lead compounds.

Table 5
Predicted drug-likeness properties of the compounds.

Compound	Mol. Wt.	Rotatable bonds	HBA	HBD	LogP	Molar Refractivity	Log K_p (cm/s)	TPSA (Å^2)
4a	320.37	3	4	2	2.70	92.21	−5.35	99.17
4b	334.39	3	4	2	2.85	97.18	−5.18	99.17
4c	350.39	4	5	2	2.87	98.70	−5.55	108.40
4d	336.37	3	5	3	2.33	94.24	−5.50	119.40
4e	335.38	3	4	3	2.25	96.62	−5.92	125.19
4f	338.36	3	5	2	2.79	92.17	−5.39	99.17
4g	354.81	3	4	2	3.02	97.22	−5.12	99.17
4h	399.26	3	4	2	3.01	99.91	−5.34	99.17
4i	388.37	4	7	2	2.86	97.21	−5.14	99.17
4j	365.37	4	6	2	2.09	101.03	−5.75	134.99
Lipinski rule	≤500	–	<10	<5	<5	40–130	–	–

4. Conclusion

In conclusion, a novel series of quinazoline-based thiazole derivatives (4a-j) were synthesized and tested for their *in vitro* anticancer activity against the cancer cell lines MCF-7, HepG2, and A549. When compared to the control, erlotinib, compounds 4g, 4i, and 4j showed significant suppression of cancer cell proliferation. The inhibitory activity of each substance was tested against wild-type, L858R/T790 M, and L858R/T790 M/C797S mutant EGFR kinases. The IC_{50} values for all of the compounds 4a-j were in the nanomolar range and showed strong kinase activity. According to the findings, compounds 4i and 4j had more EGFR kinase inhibitory effects than the standard medications staurosporine, brigatinib, and osimertinib. One of the most promising compounds, 4i has IC_{50} values of 2.17, 2.81, and 3.62 nM for inhibiting the enzymatic activity of wild-type, L858R/T790 M, and L858R/T790 M/C797S mutant EGFR kinases, respectively. Molecular docking analysis was further used to clarify and validate the mechanism of action. Through these findings, novel, very effective quinazoline-based thiazole compounds with great efficacy against cancer cell lines were found. These findings collectively imply that compound 4i would be a viable drug candidate deserving of future investigation as a new EGFR inhibitor to combat the resistance mutations EGFR-L858R/T790 M/C797S.

Funding statement

The authors extend their thanks and appreciation to Research Supporting Project (Ref: RSP2023R160) King Saud University, Riyadh, Saudi Arabia. Byong-Hun Jeon thanks Korea Institute of Energy Technology Evaluation and Planning (KETEP) grants funded by the Ministry of Trade, Industry and Energy (MOTIE) of the South Korean Govt. (No.20206410100040) for funding.

Author contribution statement

M. S. Raghu: Performed the experiments; Wrote the paper.
Swarup H A: Shamala T: Performed the experiments.
Prathibha B S: Fahd Alharethy: Analyzed and interpreted the data; Contributed reagents, materials, analysis tools or data.
K. Yogesh Kumar: Prashanth M K: Byong-Hun Jeon: Conceived and designed the experiments; Wrote the paper.

Data availability statement

No data was used for the research described in the article.

Declaration of competing interest

The authors declare that they have no known competing financial interests or personal relationships that could have appeared to influence the work reported in this paper.

Acknowledgments

The authors immensely express their indebted gratitude to the Management of BNM Institute of Technology for providing lab facilities to carry out this work. Byong-Hun Jeon thank Hanyang University, Seoul, Republic of Korea.

Appendix A. Supplementary data

Supplementary data to this article can be found online at https://doi.org/10.1016/j.heliyon.2023.e20300.

References

[1] M.A. Mohamed, R.R. Ayyad, T.Z. Shawer, A.A.M. Abdel-Aziz, A.S. El-Azab, Synthesis and antitumor evaluation of trimethoxyanilides based on 4(3H)-quinazolinone scaffolds, Eur. J. Med. Chem. 112 (2016) 106–113.
[2] C. Pottier, M. Fresnais, M. Gilon, G. Jerusalem, R. Longuespee, N.E. Sounni, Tyrosine kinase inhibitors in cancer: breakthrough and challenges of targeted therapy, Cancers 12 (2020) 731–747.
[3] M. Al-Anazi, M. Khairuddean, B.O. Al-Najjar, M.M. Alidmat, N.N.S.N. Mohamed Kamal, M. Muhamad, Synthesis, anticancer activity and docking studies of pyrazoline and pyrimidine derivatives as potential epidermal growth factor receptor (EGFR) inhibitors, Arab, J. Chem. 15 (2022), 103864.
[4] S.V. Sharma, D.W. Bell, J. Settleman, D.A. Haber, Epidermal growth factor receptor mutations in lung cancer, Nat. Rev. Cancer 7 (2007) 169–181.
[5] C.H. Yun, K.E. Mengwasser, A.V. Toms, M.S. Woo, H. Greulich, K.K. Wong, M. Meyerson, M.J. Eck, The T790M mutation in EGFR kinase causes drug resistance by increasing the affinity for ATP, Proc. Natl. Acad. Sci. U.S.A. 105 (2008) 2070–2075.
[6] A. Becker, A.V. Wijk, E.F. Smit, P.E. Postmus, Side-effects of long-term administration of erlotinib in patients with non-small cell lung cancer, J. Thorac. Oncol. 5 (2010) 1477–1480.
[7] S.S. Kaufmann, M. Pless, Acute fatal liver toxicity under erlotinib, Case Rep. Oncol. 3 (2010) 182–188.
[8] G. Stathopoulos, D. Trafalis, A. Athanasiou, G. Bardi, H. Chandrinou, Serious hematologic complications following erlotinib treatment, Anticancer Res. 30 (2010) 973–976.
[9] K. Veena, M.S. Raghu, K. Yogesh Kumar, C.B. Pradeep Kumar, F.A. Alharti, M.K. Prashanth, B.H. Jeon, Design and synthesis of novel benzimidazole linked thiazole derivatives as promising inhibitors of drug-resistant tuberculosis, J. Mol. Struct. 1269 (2022), 133822.
[10] Z. Xu, S.J. Zhao, Z.S. Lv, F. Gao, Y. Wang, F. Zhang, L. Bai, J.L. Deng, Fluoroquinolone-isatin hybrids and their biological activities, Eur. J. Med. Chem. 162 (2019) 396–406.
[11] S. Ke, L. Shi, Z. Yang, Discovery of novel isatin-dehydroepiandrosterone conjugates as potential anticancer agents, Bioorg. Med. Chem. Lett. 25 (2015) 4628–4631.
[12] M.K. Prashanth, M. Madaiah, H.D. Revanasiddappa, B. Veeresh, Synthesis, anticonvulsant, antioxidant and binding interaction of novel N-substituted methylquinazoline-2,4(1H,3H)-dione derivatives to bovine serum albumin: a structure-activity relationship study, Spectrochim. Acta, Part A 110 (2013) 324–332.
[13] M.K. Prashanth, H.D. Revanasiddappa, Synthesis of some new glutamine linked 2,3-disubstituted quinazolinone derivatives as potent antimicrobial and antioxidant agents, Med. Chem. Res. 22 (2013) 2665–2676.
[14] M.K. Prashanth, H.D. Revanasiddappa, Synthesis and antioxidant activity of novel quinazolinones functionalized with urea/thiourea/thiazole derivatives as 5-lipoxygenase inhibitors, Lett. Drug Des. Discov. 11 (2014) 712–720.
[15] H.N. Deepakumari, B.K. Jayanna, M.K. Prashanth, H.D. Revanasiddappa, B. Veeresh, Synthesis and anticonvulsant activity of N-(Substituted)-1-methyl-2,4-dioxo-1,2-dihydroquinazoline-3(4H)-carboxamides, Arch. Pharm. 349 (2016) 566–571.
[16] M.A.E.A.M. El-Hashash, M.S. Salem, S.A.M. Al-Mabrook, Synthesis and anticancer activity of novel quinazolinone and benzamide derivatives, Res. Chem. Intermed. 44 (2018) 2545–2559.
[17] S.A. Prashant, G. George, T.P. Atish, Recent advances in the pharmacological diversification of quinazoline/quinazolinone hybrids, RSC Adv. 10 (2020) 41353–41392.
[18] S.H. Ali, A.R. Sayed, Review of the synthesis and biological activity of thiazoles, Synth. Commun. 51 (2021) 670–700.
[19] F. Lemilemu, M. Bitew, T.B. Demissie, R. Eswaramoorthy, M. Endale, Synthesis, antibacterial and antioxidant activities of Thiazole-based Schiff base derivatives: a combined experimental and computational study, BMC Chemistry 15 (2021) 67.
[20] A. Petrou, M. Fesatidou, A. Geronikaki, Thiazole ring-a biologically active scaffold, Molecules 26 (2021) 3166.
[21] R. Raveesha, A.M. Anusuya, A.V. Raghu, K. Yogesh Kumar, M.G. Dileep Kumar, S.B. Benaka Prasad, M.K. Prashanth, Synthesis and characterization of novel thiazole derivatives as potential anticancer agents: molecular docking and DFT studies, Comput. Toxicol. 21 (2022), 100202.
[22] K. Veena, M.S. Raghu, K. Yogesh Kumar, K.A. Dahlous, A.A. Awadh Bahajjaj, G. Mani, Byong-Hun Jeon, M.K. Prashanth, Development of penipanoid C-inspired 2-benzoyl-1-methyl-2, 3-dihydroquinazolin-4 (1H)-one derivatives as potential EGFR inhibitors: synthesis, anticancer evaluation and molecular docking study, J. Mol. Struct. 1258 (2022), 132674.
[23] K. Yogesh Kumar, C.B. Pradeep Kumar, K.N.N. Prasad, B.H. Jeon, A. Alsalme, M.K. Prashanth, Microwave-assisted N-alkylation of amines with alcohols catalyzed by MnCl2: anticancer, docking, and DFT studies, Arch. Pharm. 355 (2022), 2100443.
[24] R. Raveesha, K. Yogesh Kumar, M.S. Raghu, S.B. Benaka Prasad, A. Alsalme, P. Krishnaiah, M.K. Prashanth, Synthesis, in silico ADME, toxicity prediction and molecular docking studies of N-substituted [1,2,4] triazolo [4,3-a] pyrazine derivatives as potential anticonvulsant agents, J. Mol. Struct. 1255 (2022), 132407.
[25] M. Madaiah, B.K. Jayanna, A.S. Manu, M.K. Prashanth, H.D. Revanasiddappa, B. Veeresh, Synthesis, characterization and evaluation of difluoropyrido[4,3-b] indoles as potential agents for acetylcholinesterase and antiamnesic Activity, Arch. Pharm. 350 (2017), e1600303.
[26] M.K. Prashanth, H.D. Revanasiddappa, K.M. Lokanatha Rai, B. Veeresh, Synthesis, characterization, antidepressant and antioxidant activity of novel piperamides bearing piperidine and piperazine analogues, Bioorg. Med. Chem. Lett. 22 (2012) 7065–7070.
[27] M. Madaiah, M.K. Prashanth, H.D. Revanasiddappa, B. Veeresh, Synthesis and evaluation of novel imidazo[4,5-c]pyridine derivatives as antimycobacterial agents against Mycobacterium tuberculosis, New J. Chem. 40 (2016) 9194–9204.
[28] M. Madaiah, M.K. Prashanth, H.D. Revanasiddappa, Novel synthesis of 4,4difluoropyrido[4,3- b]indoles via intramolecular Heck reaction, Tetrahedron Lett. 54 (2013) 1424–1427.
[29] M. Madaiah, M.K. Prashanth, H.D. Revanasiddappa, B. Veeresh, Synthesis and structure-activity relationship studies on novel 8-amino-3-[2-(4-fluorophenoxy) ethyl]-1,3-diazaspiro [4,5]decane-2,4-dione derivatives as anticonvulsant agents, Arch. Pharm. 22 (2013) 2633–2644.
[30] R. Raveesha, K. Yogesh Kumar, M.S. Raghu, S.B. Benaka Prasad, A. Ali, P. Krishnaiah, M.K. Prashanth, Synthesis, molecular docking, antimicrobial, antioxidant and anticonvulsant assessment of novel S and C-linker thiazole derivatives, Chem. Phys. Lett. 792 (2022), 139408.
[31] M.S. Raghu, C.B. Pradeep Kumar, M.K. Prashanth, K. Yogesh Kumar, B.S. Prathibha, G. Kanthimathi, S.A. Alissa, H.A. Alghulikah, S.M. Osman, Novel 1,3,5-triazine-based pyrazole derivatives as potential antitumor agents and EFGR kinase inhibitors: synthesis, cytotoxicity, DNA binding, molecular docking and DFT studies, New J. Chem. 45 (2021) 13909–13924.
[32] C.B.P. Kumar, M.S. Raghu, B.S. Prathibha, M.K. Prashanth, G. Kanthimathi, K.Y. Kumar, L. Parashuram, F.A. Alharthi, Discovery of a novel series of substituted quinolines acting as anticancer agents and selective EGFR blocker: molecular docking study, Bioorg. Med. Chem. Lett. 44 (2021), 128118.
[33] E.E. Sweeney, R.E. McDaniel, P.Y. Maximov, P. Fan, V.C. Jordan, Models and mechanisms of acquired antihormone resistance in breast cancer: significant clinical progress despite limitations, Horm. Mol. Biol. Clin. Invest. 9 (2012) 143–163.
[34] V.A. Arzumanian, O.I. Kiseleva, E.V. Poverennaya, The curious case of the HepG2 cell line: 40 Years of expertise, Int. J. Mol. Sci. 22 (2021), 13135.
[35] M. Lieber, B. Smith, A. Szakal, W. Nelson-Rees, G. Todaro, A continuous tumour-cell line from a human lung carcinoma with properties of type II alveolar epithelial cells, Int. J. Cancer 17 (1976) 62–70.
[36] W. Pao, V.A. Miller, K.A. Politi, G.J. Riely, R. Somwar, M.F. Zakowski, M.G. Kris, H. Varmus, Acquired resistance of lung adenocarcinomas to gefitinib or erlotinib is associated with a second mutation in the EGFR kinase domain, PLoS Med. 2 (2005) 225–235.
[37] K. Fu, F. Xie, F. Wang, L. Fu, Therapeutic strategies for EGFR-mutated non-small cell lung cancer patients with osimertinib resistance, J. Hematol. Oncol. 15 (2022) 173.
[38] C.A. Eberlein, D. Stetson, A.A. Markovets, K.J. Al-Kadhimi, Z. Lai, P.R. Fisher, C.B. Meador, P. Spitzler, E. Ichihara, S.J. Ross, M.J. Ahdesmaki, A. Ahmed, L. E. Ratcliffe, E.L. O'Brien, C.H. Barnes, H. Brown, P.D. Smith, J.R. Dry, G. Beran, K.S. Thress, B. Dougherty, W. Pao, D.A. Cross, Acquired resistance to the mutant-selective EGFR inhibitor AZD9291 is associated with increased dependence on RAS signalling in preclinical models, Cancer Res. 75 (2015) 2489–2500.
[39] H. Zhang, H.Y. Zhao, X.X. Xi, Y.J. Liu, M. Xin, S. Mao, J.J. Zhang, A.X. Lu, S.Q. Zhang, Discovery of potent epidermal growth factor receptor (EGFR) degraders by proteolysis targeting chimera (PROTAC), Eur. J. Med. Chem. 189 (2020), 112061.

[40] R. Thomas, Z. Weihua, Rethink of EGFR in cancer with its kinase independent function on board, Front. Oncol. 9 (2019) 800.
[41] Q. Liu, S. Yu, W. Zhao, S. Qin, Q. Chu, K. Wu, EGFR-TKIs resistance via EGFR-independent signalling pathways, Mol. Cancer 17 (2018) 53.
[42] K. Shi, G. Wang, J. Pei, J. Zhang, J. Wang, L. Ouyang, Y. Wang, W. Li, Emerging strategies to overcome resistance to third-generation EGFR inhibitors, J. Hematol. Oncol. 15 (2022) 94.
[43] C.A. Lipinski, F. Lombardo, B.W. Dominy, P.J. Feeney, Experimental and computational approaches to estimate solubility and permeability in drug discovery and development settings, Adv. Drug Deliv. Rev. 64 (2012) 4–17.
[44] G. Vistoli, A. Pedretti, B. Testa, Assessing drug-likeness–what are we missing? Drug Discov. Today 13 (2008) 285–294.